Research on the Influence of Different Coiling Methods of High-Voltage Cables on Magnetic Field Distribution in Fully Mechanized Coal Mining Face

¹Bao Liu and ²Jialu Liu,

^{1,2}School of Mechanical and Power Engineering, Henan Polytechnic University, Jiaozuo, China

Abstract: This paper addresses the issue of changes in magnetic field distribution caused by different coiling methods during the recovery of high-voltage cables in fully mechanized coal mining face underground. We used simulation software to analyze the magnetic field distribution of three-core cables under different coiling states. The results show that the magnetic field under multi-loop circular coiling exhibits a complex three-dimensional non-axisymmetric structure, while in figure-8 coiling, the magnetic field is enhanced due to superposition at the central intersection point where the current directions are the same. The magnetic field strengths at the center of the coils are similar for both coiling methods, but differences exist in the lateral magnetic field distribution. This study provides a theoretical basis for the safe recovery of cables and the evaluation of magnetic field effects.

Keywords: Underground coal mine; Three-core cable; Finite element; Electromagnetic radiation

I. INTRODUCTION

In the fully mechanized mining face of coal mines, various production equipment require cable power supply[1]. As the mining face advances, cables tend to accumulate. To ensure uninterrupted operation of the coal mining machine, the cable to be retrieved is connected to the power supply equipment at one end, meanwhile the opposite end is linked to the face mobile transformer or directly integrated with the shearer. With both ends of the cable fixed, the coiling of redundant cables due to the retreat of the mining face can only be performed on the middle section of the cable.

The mainstream coiling methods for underground cables currently include direct circular coiling (coiling in the same direction) and figure-8 coiling. Among these, figure-8 coiling is an important method for coiling redundant high-voltage cables in a compact storage space when both ends of the cable are fixed in the fully mechanized mining face. This method is employed to avoid excessive torsion caused by same-direction spiral winding. Compared to direct circular coiling, the figure-8 coiling method effectively counteracts the residual torsion in the coiled cable, thereby extending the cable's service life. As a result, figure-8 coiling has become the primary method for coiling redundant cables in fully mechanized mining faces.

Different coiling methods cause the cable to exhibit varying deformation states, leading to differences in the magnetic field distribution of the cable. Existing analytical calculations for cable distribution parameters face challenges such as complex implementation processes, limited accuracy in parameter extraction, and inadequacy for addressing large deformations during cable recovery[2]. To tackle these issues, this study proposes the use of finite element analysis software to analyze the magnetic field distribution during the cable recovery

process, taking into account different coiling methods.

II. 2D CABLE MAGNETIC FIELD ANALYSIS

A. Principle of Surface Magnetic Field Calculation for Three-Core Cable

The relationship linking the magnetic field and current is given by the differential form of Ampère's circuital law:

$$\nabla \times H = J \tag{1}$$

Where: H is the magnetic field strength; J is the conduction current density. This equation indicates that the curl of the magnetic field strength H at a point in a magnetic medium equals the conduction current density at that point.

According to the magnetic vector potential and the characteristics of magnetostatic fields:

$$B = \nabla \times A \tag{2}$$

Where: B is the magnetic flux density; A is the magnetic vector potential.

According to Maxwell's equations:

$$E = -j\omega A \tag{3}$$

$$I = \int_{S} J \cdot dS \tag{4}$$

Where: E is the electric field strength; ω is the angular frequency; I is the current; S is the area through which the current passes. The current through area S equals the flux of the current density over S. This establishes the relationship between current and magnetic field, providing a theoretical basis for current detection in three-core cables based on magnetic field inversion[3].

B. Simulation Modeling of the Three-Core Cable

Taking a 10kV metal-shielded monitoring rubber-sheathed flexible cable as an example, appropriate simplifications were made to the materials during modeling, such as replacing actual filling materials in the cable model (e.g., PVC, PE) with air[4]. These material simplifications do not affect the analysis of magnetic field distribution while simplifying the model structure and improving computational efficiency. The geometric configuration of the cable modeling is shown in Figure 1, with specific parameters listed in Table 1.

International Journal of Trend in Research and Development, Volume 12(6), ISSN: 2394-9333 www.ijtrd.com

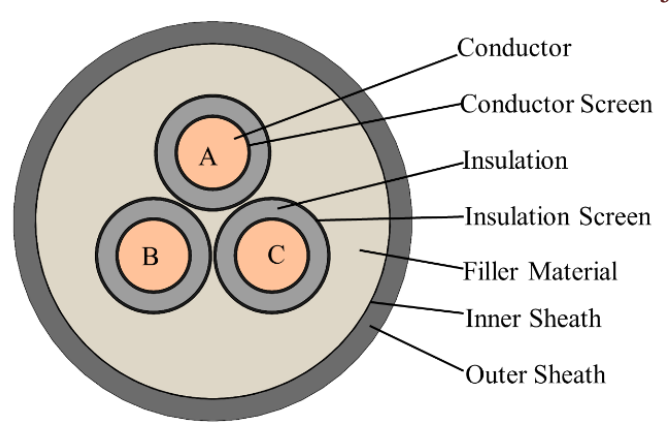


Figure 1:Simplified planar geometric configuration of the cable model.

Table 1 Structural Parameters of 10kV High-Voltage Cable

Name	Value (mm)
Conductor Diameter	17.8
Inner Sheath Thickness	3
Outer Sheath Thickness	5.5
Cable Outer Diameter	101.1

During steady-state operation, the 10kV three-core cable carries the following three-phase currents[5]:

$$\begin{cases} I_A = 300\sqrt{2}\sin(100\pi t) \\ I_B = 300\sqrt{2}\sin(100\pi t - \frac{2\pi}{3}) \\ I_C = 300\sqrt{2}\sin(100\pi t + \frac{2\pi}{3}) \end{cases}$$
 (5)

C. Two-Dimensional Cable Cross-Section Magnetic Field Distribution

The cable magnetic field distribution is shown in Figure 2. Unlike a single-core cable, the magnetic flux lines of a three-core cable are not symmetrical circles but elliptical shapes surrounding the cable conductors.

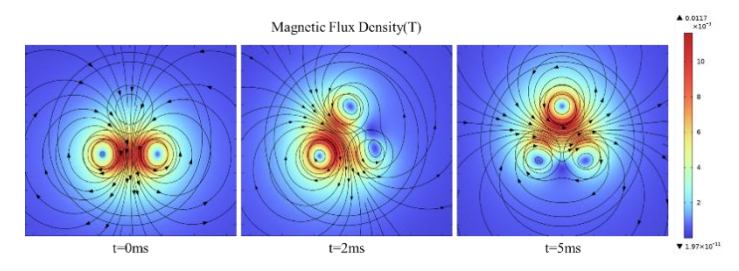


Figure 2:Cable magnetic field distribution at three different time instants.

Observing Figure 2, it is evident that the magnetic field distribution inside the cable differs at different time instants. Unlike the electric field distribution, the magnetic fields of the three phases are not independent but interact with each other. At t=0ms in Figure 2, the maximum magnetic flux density appears between phases B and C because the currents in these two phases are equal in magnitude but opposite in direction, leading to magnetic field superposition and an increase in magnetic flux density at that location. The magnetic field near phase A is relatively small, largely because the current in phase A is zero at this moment, and it is farther away from phases B and C, resulting in lower magnetic flux density. At t=5ms, the position

of maximum magnetic flux density appears within phase A, Inclined toward the center of the entire three-core cable. This is because phase A itself carries a relatively large current, compounded by the influence of phases B and C, whose currents are opposite in direction to phase A, leading to superimposed magnetic flux density and a maximum value at this point. It can also be observed from the figure that the minimum point of magnetic flux density occurs at the filler layer where the magnetic fields of phases B and C intersect. This is because the currents in these two phases are equal in magnitude and direction, producing magnetic fields in opposite directions that cancel each other upon superposition, reducing the magnetic flux density.

II. MAGNETIC FIELD ANALYSIS OF CABLES WITH DIFFERENT WINDING METHODS

A. Magnetic Field Distribution of Circularly Coiled Cable

To simulate actual retrieval conditions, a three-dimensional model of a cable coiled in three turns was established, as shown in Figure 3. Model parameters were set according to common underground practices to reflect the accumulation and distribution effects of the magnetic field in space.



Figure 3:Three-dimensional modeling of multi-turn circular coiling.

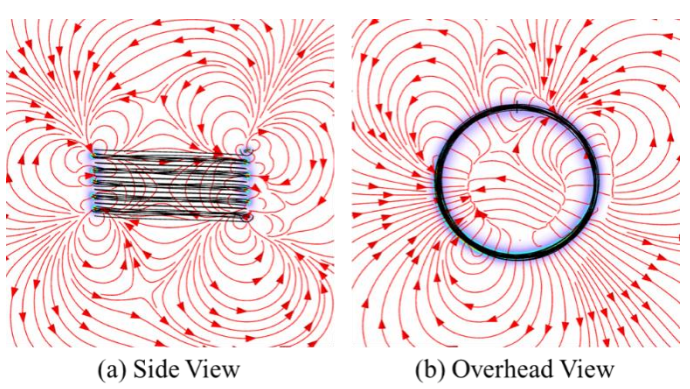


Figure 4:Magnetic field distribution of the multi-turn circularly coiled three-phase cable.

From Figure 4, it can be seen that the magnetic field magnitude at the middle cross-section of the circularly coiled cable exhibits high values at the top and bottom edges and a lower value in the middle. This is because the current direction is the same in every turn of the circular coil. This causes the magnetic fields from the cable in the middle and its adjacent cables to be in opposite directions, leading to mutual cancellation and resulting in a lower magnetic field magnitude in the middle compared to the edges.

B. Magnetic Field Distribution of Figure-8 Coiled Cable

Similarly, a three-dimensional model of a cable wound in a "figure-8" pattern with three complete "figure-8" units was established, as shown in Figure 5. This model can clearly demonstrate the superimposed influence of multiple crossover points on the magnetic field.

International Journal of Trend in Research and Development, Volume 12(6), ISSN: 2394-9333 www.ijtrd.com



Figure 5:Three-dimensional modeling of multi-turn figure-8 coiled cable.

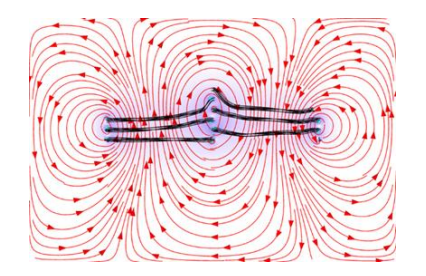


Figure 6: Side view of magnetic field distribution for multi-turn figure-8 coiled three-phase cable.

Through Figure 6,Due to the mutual superposition of magnetic fields between each loop, the magnetic field strength is greater, and the magnetic field lines are denser. The side magnetic field exhibits three vortex-like shapes.

C. Comparison of Magnetic Field Distribution and Magnitude between Circular Coiling and Figure-8 Coiling

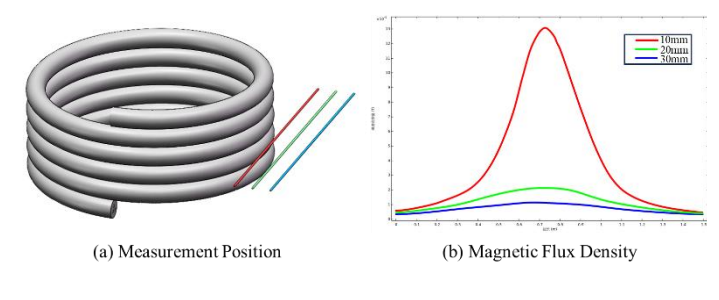


Figure 7: Lateral horizontal line magnetic field strength for multi-turn circularly coiled three-phase cable.

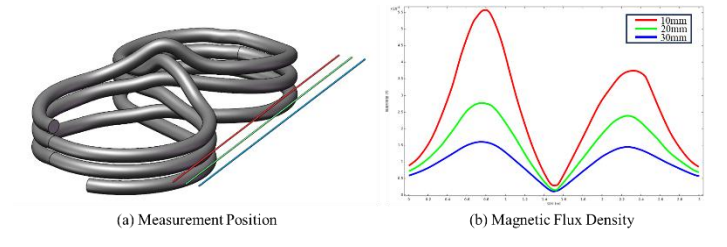


Figure 8: Lateral horizontal line magnetic field strength for multi-turn figure-8 coiled three-phase cable.

As shown in Figures 7 and 8, the magnetic field strength around multi-turn circularly coiled and multi-turn figure-8 coiled cables was measured. Straight lines were drawn on the plane of the cable coil at distances of 10cm, 20cm, and 30cm from the cable. The magnetic field strength along these lines was plotted and compared.

From the figures, it can be seen that the maximum magnetic field generated by the multi-turn figure-8 coiling method is several times larger than that of the multi-turn circular coiling method. Comparing the magnetic field strengths at different distances reveals that the magnetic field strength of the multi-turn figure-8 coil decays more slowly. For the circular coil, the magnetic field beyond 30cm has decayed to less than

one-tenth of the maximum value, whereas for the figure-8 coiled cable, the magnetic field strength at 30cm has only decayed to about one-third of its value at 10cm. This is because the magnetic field energy is more concentrated in the figure-8 configuration, resulting in slower near-field decay.

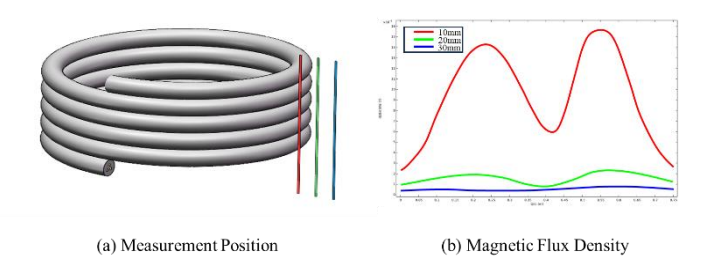


Figure 9: Lateral vertical line magnetic field strength for multi-turn circularly coiled three-phase cable.

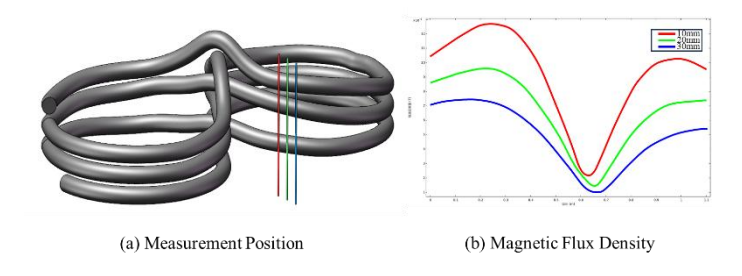


Figure 10: Lateral vertical line magnetic field strength for multi-turn figure-8 coiled three-phase cable.

As shown in Figures 9 and 10, the magnetic field strength in the lateral vertical direction for multi-turn circularly coiled and multi-turn figure-8 coiled cables was measured. Straight lines were drawn on the plane of the cable coil at distances of 10cm, 20cm, and 30cm from the cable. The magnetic field strength along these lines was plotted and compared.

The patterns in magnetic field magnitude distribution for the two coiling methods are similar to those analyzed above. However, their magnetic field distribution curves exhibit different characteristics, showing a pattern of high on both sides and low in the middle. This is caused by the mutual cancellation of magnetic fields from the cables in the middle of the multi-turn coil. In terms of magnetic field magnitude, the multi-turn circular coil has a slightly higher magnetic field strength than the multi-turn figure-8 coil, because the sampling line is closer in linear distance to the circularly coiled cable. Regarding the magnetic field decay rate, the multi-turn circular coil decays much faster than the multi-turn figure-8 coil.

CONCLUSION

By establishing refined models of multi-turn circular and multi-turn figure-8 coiled cables, this study has quantitatively compared their three-dimensional magnetic field distributions. The results indicate that under multi-turn coiling conditions, the figure-8 method produces an average magnetic field strength on the cable side that is more than 3 times higher than the circular method, with a slower decay rate. A significant magnetic field concentration effect was observed at the structural crossover points, where the local strength reached $3.20{\times}10^{-4}$ T.

Therefore, during underground cable retrieval operations where control of the surrounding electromagnetic environment is necessary, the circular coiling method should be prioritized. If figure-8 coiling is adopted, the crossover points should be avoided from facing sensitive areas to minimize

International Journal of Trend in Research and Development, Volume 12(6), ISSN: 2394-9333 www.ijtrd.com

electromagnetic influence.

These findings not only deepen the theoretical understanding of electromagnetic field behavior in multi-conductor systems under complex shapes but also provide an important reference basis for the safe retrieval operation of cables in underground coal mines in engineering practice. Optimizing the coiling method has positive guiding significance for assessing and controlling the electromagnetic environment around cables, preventing potential electromagnetic interference, and ensuring underground safety production.

References

- [1] FU Wenjun, REN Qiang, ZHANG Liang. Study on safety and reliability of power supply to fully mechanized coal mining face in Hongqingliang Coal Mine[J]. Mine Construction Technology, 2020, 41(1): 57-60.
- [2] LI Shisong, YUAN Yanling, DONG Jie, et al. An analytical method for calculating surface magnetic field of three-core power cables[J]. China Measurement & Test, 2017, 43(4): 95-99.
- [3] XIE Kun, ZHANG Wei, ZHANG Jie, et al. Research on physico-chemical and electrical properties of insulation in high-voltage cable accessories[J]. Advanced Technology of Electrical Engineering and Energy, 2022, 41(1): 81-86.
- [4] SU Jingang, ZHANG Peng, HUANG Xingwang, et al. Simulation research on non-contact current measurement of three-core cable based on magnetic field inversion[J]. Hebei Electric Power Technology, 2024, 43(03): 50-54. [DOI:CNKI:SUN:HBJS.0.2024-03-009]
- [5] SHE Xiaolong, ZHUO Chao, ZENG Jupeng, et al. Current measurement method for cores and metal sheath of three-core cable based on electromagnetic analysis method[J]. Proceedings of the CSU-EPSA, 2025, 37(09): 149-158. [DOI:10.19635/j.cnki.csu-epsa.001558].